Scripta Materialia 130 (2017) 178–181

Contents lists available at ScienceDirect

Scripta Materialia

journal homepage: www.elsevier.com/locate/scriptamat

Regular article

Shear strengths of FCC-FCC cube-on-cube interfaces

Xuying Liu, Rui Hao, Shimin Mao, Shen J. Dillon *

Department of Materials Science and Engineering, University of Illinois at Urbana Champaign, 1304 West Green Street, Urbana, IL 61801, United States

ARTICLE INFO

Article history:
Received 3 August 2016
Received in revised form 28 November 2016
Accepted 29 November 2016
Available online xxxx

Keywords:
Shear strength
Interfaces
Multilayers
In situ
Transmission electron microscopy

ABSTRACT

This work employs in-situ transmission electron microscopy based nanopillar compression of physical vapor deposited multilayers to measure the interfacial shear strengths of model Ag-Pd, Ag-Au, Ag-Ni, Ag-Cu, and Cu-Ni (111) oriented cube-on-cube interfaces. The experimental trends are primarily rationalized by considering the coherency regimes. Coherent interfaces shear via slip transmission across them. Pillars containing semi-coherent interfaces with <5% atomic misfit deform rather homogeneously. Interfaces exhibiting atomic misfit >5% shear locally and their interfacial shear strength decreases with increasing misfit.

Interfaces often dominate plastic response of nanostructured alloys, and thus engineering metals to introduce controlled interfacial properties is a key goal in alloy design. In multiphase systems, significant effort has been made to understand how dislocations interact with interfaces [1]. Multilayered nanocomposite materials have received significant attention as model systems that can be fabricated in bulk and have excellent mechanical properties [2,3], thermal stability, and radiation resistance [4,5]. It has been suggested that the maximum shear strength achievable in such multilayers occurs when a confined layer slip mechanism transitions to slip transmission of single dislocations [1]. Computational efforts have revealed the nature of dislocation interactions at such heterophase interfaces; including slip transition, and interfacial sliding [1,6,7]. We refer the reader to recent reviews by Wang and Misra [8], Wang et al. [9] and Hoagland et al. [7] that discuss the properties and mechanical response of coherent and incoherent interfaces. It has been suggested that when interfacial shear strength is low, slip transition across FCC-BCC interfaces is difficult and thus the yield stress of the bulk nanolaminates is high. For example, previous nanocompression experiments on Cu-Nb multilayers demonstrated that the interfacial shear strength is in the range of 0.3–0.6 GPa, while the yield strength of the system is as high as 2.5 GPa [10]. The influence of atomic bonding was treated by constructing molecular dynamics simulations of FCC-BCC systems where the components A and B have the bulk properties of Cu and Nb, but the heats of mixing, i.e. A-B bond energy were varied [11]. The interfacial shear strength decreased with increased heat of mixing [11]. In support of their results, Al-Nb which has a negative heat of mixing, was shown via experiment to have a much lower yield stress than Cu-Nb of similar layer thickness [12]. The inverse correlation between heat of mixing and interfacial shear strength could be an important system design criterion, but this remains to be confirmed experimentally. The authors themselves noted that this rule may only apply to the very specific interface type and chemistry treated [11]. It is also anticipated that constitutional interface dislocations necessary to relax coherency strains should affect the interfacial shear strength as well, as described in Ref [1]. Recently, Zeng et al. [13] used molecular dynamics to treat dislocation slip transmission across a number of distinct interfaces. Due to the complex and directionally anisotropic nature of the interface-dislocation interactions, as well as the dual importance of structural and chemical aspects of the interfacial bonding, the authors were not able to isolate a single parameter that ideally captured the trends in the data. However, they suggested that the energy of the residual dislocation at the interface is the best description of critical stress for slip transmission across the interface. While computational methods have been applied to calculating the effects of interfacial structure and chemistry on slip transmission, interfacial shearing, and mechanical properties of nanolaminates, complementary experimental validation remains limited. This work specifically seeks to experimentally quantify the deformation response of nanolaminates whose structure and chemistry are varied systematically.

In this work, we characterize the interfacial shear strength of Ag-X interfaces, where X = Pd, Cu, Ni, and Au whose heats of mixing are $\Delta H_{Ag-Pd} \approx -4.8$ kJ/mol [14], $\Delta H_{Ag-Au} \approx -4.6$ kJ/mol [15], $\Delta H_{Ag-Cu} \approx 6$ kJ/mol [16], and $\Delta H_{Ag-Ni} \approx 20$ kJ/mol [17]. The atomic misfit strains between these materials are 5%, 0%, 11%, and 14%, respectively. We chose FCC-FCC systems to have a common Ag component layer, vary from miscible to highly immiscible, and exhibit different atomic misfit strains. Samples of this type can be grown via physical vapor deposition to have cube-on-cube misorientations, with (111) interfaces. These

* Corresponding author.
E-mail address: sdillon@illinois.edu (S.J. Dillon).

http://dx.doi.org/10.1016/j.scriptamat.2016.11.038
1359-6462/

factors allow us to experimentally probe the trends in the interfacial shear strength as a function of relevant variables. The interfacial shear strength is tested via in-situ transmission electron microscopy (TEM) based nanocompression, since prior studies indicate the utility of the approach for identifying the exact stress at which interfaces begin to shear [18]. Additionally, we test Cu-Ni as a model system that exhibits both a small positive heat of mixing and small misfit ($\Delta H_{Cu-Ni} \approx 2.9$ kJ/mol and $\Delta a_o \approx 3\%$). The data are then compared with our prior measurements of FCC/BCC interfaces [4].

Multilayer nanolaminates were grown on pre-tilt substrates to enhance the resolved shear stress on the interface. A focused ion beam (FIB, FEI DUAL BEAM 235) was used to mill platforms 6 μm × 7 μm at pre-tilt angles of 30°, 45° or 60° on Si platform substrates (Hysitron, Minneapolis). Different angles were tested to ensure a consistent measure of the interfacial shear strength, which will be independent of tilt angle if interfacial roughness is not a dominant factor. Multilayers of Ag (99.99%, Kurt, J. Lesker, Jefferson Hills)–Ni (99.99%, Lesker), Ag-Pd (99.95%, Lesker), Ag-Cu (99.99%, Lesker), Ag-Au (99.99%, Lesker), and Cu-Ni were grown on these platforms by Magnetron Sputtering (AJA International INC. N Scituate) under 3 mTorr Ar with a base pressure below 10^{-6} Torr. The thickness of each layer was ≈50 nm and the total thickness of the laminates were ≈1.5 μm. The samples were then attached to a Cu mount that holds the sample in the Hysitron Picoindenter PI-95. Pillars were subsequently cut to their final diameter; ≈200 nm with aspect ratios of ≈2:1–3:1 by FIB (FEI Helios 600i). The top of each pillar was cut to provide a flat contact surface for subsequent nanocompression testing. After calibration of the indenter, pillars were compressed in displacement-control mode at a rate of 1 nm s^{-1} with a 2 μm diameter flat diamond punch. At least 3 pillars were tested to provide a mean value of the shear strength and an experimental standard deviation. Since the pillars are too thick to allow satisfactory characterization of the microstructure, thin cross-sections were also prepared from the pristine samples and characterized by TEM (JOEL 2010F, 200 kV). Fig. 1 shows the TEM images of Ag-Cu, Ag-Ni, Ag-Pd, and Ag-Au interfaces. The in-plane grain size in each sample is ≈100 nm, thus each pillar contains multiple grains and the measured shear strengths will be averaged over several slip directions. Such nanograined multilayers do not exhibit pillar diameter size effects in this range as demonstrated in prior work [4].

Fig. 2 shows example nanocompression results for each of the four Ag-X systems. Several of the samples were tested to strains where shearing occurred at multiple interfaces within the sample. Since the pillars are slightly tapered, interfaces with the smallest cross-sectional area shear first at lower loads, followed by larger area interfaces at higher loads. Overall, the stress at which different interfaces shear within the same sample varies by at most 13%. The variation in stress at which interfaces shear between different samples of the same chemistry is ≈14%. In Ag-Cu and Ag-Ni, there is a load drop associated with the onset of irreversible interfacial shearing, since the cross-sectional area is reduced during interfacial sliding and plasticity is localized at the interface. In Ag-Pd partial interfacial shearing is observed at the onset of plastic deformation, but the interfaces do not shear completely and no associated stress drop occurs. This suggests that

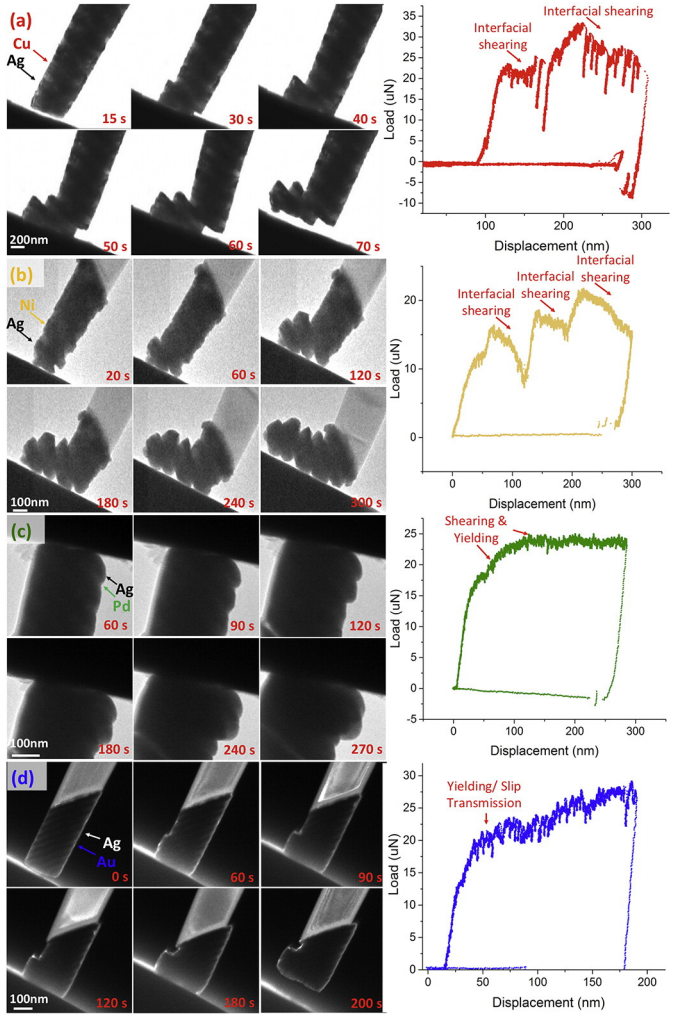

Fig. 2. Time-lapse TEM images and load-displacement curves corresponding to in-situ nanocompression of (a) Ag-Cu, (b) Ag-Ni, (c) Ag-Pd, and (d) Ag-Au samples. (d) is imaged in dark-field TEM while the rest are shown in bright-field.

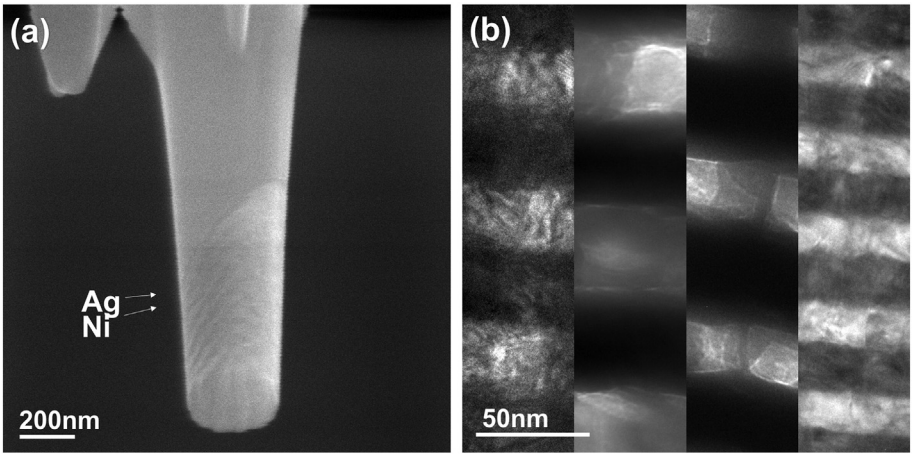

Fig. 1. (a) SEM image of Ag-Ni pillar before compression. (b) 150K bright-field cross-sectional TEM image of an Ag-Cu, Ag-Ni, Ag-Pd, and Ag-Au multilayer.

bulk deformation is active in these samples and that while plasticity initiates with some interfacial sliding, the shear strength is comparable to the bulk yield strength. The Ag-Au interfaces do not shear and the pillars do not deform uniformly. Instead, the sample shears at a 45° angle with shearing occurring normal to the interfaces. This indicates that slip transmission across the interface is most favorable in Ag-Au.

To calculate the interfacial shear strength, τ, from the load at yield, F, we employ the Schmid factor:

$$\tau = \frac{\text{resolved force acting on slip plane}}{\text{area of slip plane}} = \frac{F\cos\lambda}{\pi R^2/\cos\phi} = \frac{F\cos\lambda\cos\phi}{\pi R^2} \quad (1)$$

where R is the radius of the pillar (averaged between the radius measured at the top and bottom of the shearing layer), ϕ is the inclination angle of the interface away from the loading axis, and λ is the angle of the glide direction in plane. The angle ϕ is measured from the experimental images, as is R. The interfacial shear strength values obtained from application of the Schmid factor to the experimental data are as follows; Ag-Cu has the lowest interfacial shear strength, 0.30 ± 0.04 GPa, followed by Ag-Ni 0.53 ± 0.08 GPa, and Ag-Pd 1.1 ± 0.1 GPa. Ag-Au likely exhibits the highest shear strength since it does not shear along the interface, instead it prefers shearing in the direction perpendicular to the interface, which produces a yield strength of 0.38 ± 0.02 GPa. Since the measured values differ significantly, the values must be associated with the mechanical characteristics of the interface rather than with that of the softest phase, Ag, in each. $\tau_{Ag-Cu} < \tau_{Ag-Ni} < \tau_{Ag-Pd} < \tau_{Ag-Au}$ and $\Delta H^{mix}_{Ag-Ni} > \Delta H^{mix}_{Ag-Cu} > \Delta H^{mix}_{Ag-Au} > \Delta H^{mix}_{Ag-Pd}$; no trend exists between heats of mixing and the interfacial shear strengths, as is summarized in Table 1. Adding Cu-Ni to the comparison, it is noted that the misfit strain at the Ag-Pd, Ag-Au, and Cu-Ni interfaces are smaller than Ag-Cu and Ag-Ni, while Ag-Ni and Ag-Cu are quite similar. It has been suggested that the shear strength and slip transmission stress should show an inverse relationship. Recent computational work suggests that the slip transmission stress correlates well with the energy of the remnant partial dislocation existing at the interface after the slip transmission event. A linear elastic approximation of this energy was provided

$$\psi = \frac{a^{(2)}G^{(2)}}{a^{(1)}G^{(2)}}\left(\frac{a^{(1)}}{a^{(2)}} - \frac{G^{(1)}}{G^{(2)}}\right)^2 \quad (2)$$

where a is the lattice parameter and G is the shear modulus [13]. Again, we do not find an ideal correlation between this parameter and our experimental measurements (see Table 1). However, this may still be reasonable since the proposed relationship between slip transmission stress and interfacial shear strength is qualitative.

The atomic misfit should affect the interfacial shear strength and conditions for slip transmission, since it defines the equilibrium interfacial dislocation content [19,20]. Fig. 3 plots the yields strengths and interfacial shear strengths of the multilayers versus atomic misfit. Atomic misfit <5% is often considered to be semi-coherent, while greater misfit is often classified as incoherent [8]. Ag-Au, Cu-Ni, and Ag-Pd

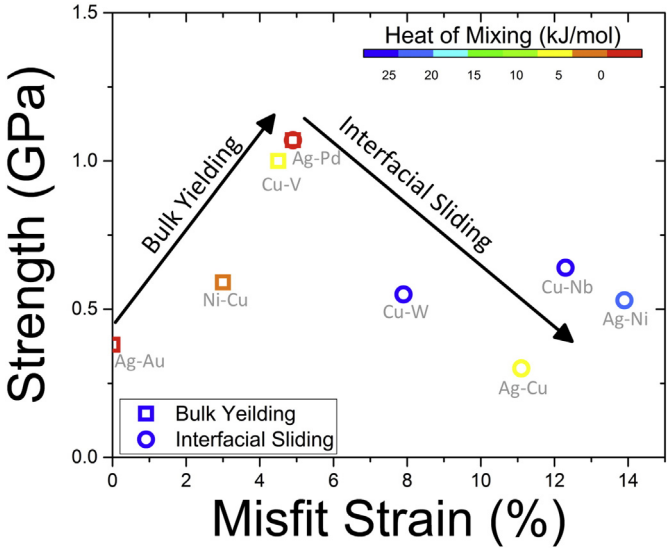

Fig. 3. Summary of the strength data as a function of atomic misfit, which shows a transition from yielding to interfacial sliding at ≈5% misfit. The data is colored by the A–B heats of mixing. (For interpretation of the references to color in this figure legend, the reader is referred to the web version of this article.)

interfaces can be classified as semi-coherent, with 0%, 3%, and 4.9% misfit, with the latter existing at the nominal boundary. The results of the compression tests reveal that only Ag-Pd interfaces exhibit any shearing behavior. The Ni-Cu interfaces do not shear at all and Ag-Au interfaces enable easy slip transfer. Interfaces with atomic misfit >5% all undergo interfacial shearing. On average the shear strength tends to decrease with increasing atomic misfit, although there is scatter in the data, which likely reflects differences in chemical interactions. However, we do not find good correlations with simple single descriptors of chemical interactions such as heats of mixing or A-B bonding energies. Overall, our experimental results suggest that both structural and chemical aspects of interfacial bonding influence the quantitative details of interfacial mechanical properties, while atomic misfit dominates the preferred deformation modes.

1. Conclusions

In this work, interfacial shear at different (111) FCC-FCC cube-on-cube interfaces has been systematically quantified experimentally. A maximum overall compressive strength occurs for samples with atomic misfit of ≈5% where neither slip transmission or interfacial shearing are clearly preferred. No single descriptor of the system captures the experimental trends, but both chemical bonding and atomic misfit appear to be important factors, with the latter strongly influencing the preferred deformation mode. Transitions from preferential interfacial sliding, to bulk deformation, and finally to slip transmission occur with decreasing amounts of interfacial atomic misfit.

Table 1
Misfit, bonding energy calculated from a regular solution model, shear strength and heat of mixing of all the FCC/FCC and FCC/BCC systems investigated. Note that for calculating the yield stress, we utilized the same Schmid factor in the analysis to aid comparison of the data.

Interfaces	misfit/%	Bonding energy/kJ/mol	Yield strength/GPa	Shear strength/GPa	Standard deviation/GPa	Heat of mixing/kJ/mol	Residual dislocation parameter, ψ
Ag-Au	0	52.84	0.38 (Slip transmission)	Yields	0.02	−4.6 [15]	0.16
Cu-Ni	3	62.62	0.58	Yields	0.09	2.9 [21]	5.90
Cu-V	4.5	93.21	1.0	Yields	0.1	5 [22]	0.51
Ag-Pd	4.9	56.42	Shears & yields	1.1	0.1	−4.8 [14]	3.01
Cu-W	7.9	131.64	Shears	0.55	0.1	24 [23]	53.4
Ag-Cu	11.1	49.49	Shears	0.30	0.04	6 [16]	5.81
Ag-Ni	13.9	52.44	Shears	0.53	0.08	20 [17]	20.9
Cu-Nb	12.3	113.23	Shears	0.60	0.05	28 [24]	0.39

Acknowledgements

X.L. and S.M were supported by the US DOE-BES under grant DEFG02-05ER46217. R.H. was supported by the ONR-MURI under the grant no. N00014-11-1-0678.

Reference

[1] H.M. Zbib, C.T. Overman, F. Akasheh, D. Bahr, Int. J. Plast. 27 (2011) 1618–1639, http://dx.doi.org/10.1016/j.ijplas.2011.03.006.
[2] Y. Chen, Y. Liu, C. Sun, K.Y. Yu, M. Song, H. Wang, X. Zhang, Acta Mater. 60 (2012) 6312–6321, http://dx.doi.org/10.1016/j.actamat.2012.08.005.
[3] Y.-C. Wang, A. Misra, R.G. Hoagland, Scr. Mater. 54 (2006) 1593–1598, http://dx.doi.org/10.1016/j.scriptamat.2006.01.027.
[4] S. Mao, S. Özerinç, W.P. King, R.S. Averback, S.J. Dillon, Scr. Mater. 90 (2014) 29–32, http://dx.doi.org/10.1016/j.scriptamat.2014.07.009.
[5] A. Misra, J.P. Hirth, R.G. Hoagland, Acta Mater. 53 (2005) 4817–4824, http://dx.doi.org/10.1016/j.actamat.2005.06.025.
[6] J. Wang, C. Zhou, I.J. Beyerlein, S. Shao, JOM 66 (2014) 102–113.
[7] R.G. Hoagland, R.J. Kurtz, C.H. Henager, Scr. Mater. 50 (2004) 775–779, http://dx.doi.org/10.1016/j.scriptamat.2003.11.059.
[8] J. Wang, A. Misra, Curr. Opin. Solid State Mater. Sci. 15 (2011) 20–28, http://dx.doi.org/10.1016/j.cossms.2010.09.002.
[9] J. Wang, A. Misra, R.G. Hoagland, J.P. Hirth, Acta Mater. 60 (2012) 1503–1513, http://dx.doi.org/10.1016/j.actamat.2011.11.047.
[10] N. Li, N.A. Mara, J. Wang, P. Dickerson, J.Y. Huang, A. Misra, Scr. Mater. 67 (2012) 479–482, http://dx.doi.org/10.1016/j.scriptamat.2012.06.008.
[11] X.-Y. Liu, R.G. Hoagland, J. Wang, T.C. Germann, A. Misra, Acta Mater. 58 (2010) 4549–4557, http://dx.doi.org/10.1016/j.actamat.2010.05.008.
[12] E.G. Fu, N. Li, A. Misra, R.G. Hoagland, Mater. Sci. Eng. A 493 (2008) 283–287, http://dx.doi.org/10.1016/j.msea.2007.07.101.
[13] Y. Zeng, A. Hunter, I.J. Beyerlein, M. Koslowski, Int. J. Plast. 79 (2016) 293–313, http://dx.doi.org/10.1016/j.ijplas.2015.09.001.
[14] C. Luef, A. Paul, H. Flandorfer, A. Kodentsov, H. Ipser, J. Alloys Compd. 391 (2005) 67–76, http://dx.doi.org/10.1016/j.jallcom.2004.08.056.
[15] R.R. Hultgren, Selected Values of Thermodynamic Properties of Metals and Alloys, Wiley, New York, 1963.
[16] T. Klassen, U. Herr, R.S. Averback, Acta Mater. 45 (1997) 2921–2930, http://dx.doi.org/10.1016/S1359-6454(96)00388-6.
[17] J. Xu, U. Herr, T. Klassen, R.S. Averback, J. Appl. Phys. 79 (1996)http://dx.doi.org/10.1063/1.361820.
[18] N.A. Mara, D. Bhattacharyya, P. Dickerson, R.G. Hoagland, A. Misra, Appl. Phys. Lett. 92 (2008)http://dx.doi.org/10.1063/1.2938921.
[19] W.P. Vellinga, J.T.M. De Hosson, V. Vitek, Acta Mater. 45 (1997) 1525–1534, http://dx.doi.org/10.1016/S1359-6454(96)00279-0.
[20] J.T.M. de Hosson, H.B. Groen, B.J. Kooi, V. Vitek, Acta Mater. 47 (1999) 4077–4092, http://dx.doi.org/10.1016/S1359-6454(99)00268-2.
[21] V.T. Witusiewicz, F. Sommer, Metall. Mater. Trans. B Process Metall. Mater. Process. Sci. 31 (2000) 277–284, http://dx.doi.org/10.1007/s11663-000-0046-7.
[22] U. Mizutani, C.H. Lee, Mater. Trans. JIM 36 (1995) 210–217, http://dx.doi.org/10.2320/matertrans1989.36.210.
[23] M. Nastasi, F.W. Saris, L.S. Hung, J.W. Mayer, J. Appl. Phys. 58 (1985)http://dx.doi.org/10.1063/1.335855.
[24] E. Botcharova, J. Freudenberger, L. Schultz, Acta Mater. 54 (2006) 3333–3341, http://dx.doi.org/10.1016/j.actamat.2006.03.021.